UDC 661.892:544.223.22

C. Z. Fan, J. Li, M. Hu (Qinhuangdao, PR China)
Z. S. Zhao (Washington, USA)
B. Xu, J. L. He (Qinhuangdao, PR China)

A novel layer-structured PtN_2: first-principles calculations

Platinum nitride as the first successfully synthesized noble metal nitride shows superior mechanical properties and exotic electronic structure that rival those of conventional transition metal nitrides. In the past diverse crystal structures have been proposed to understand its unusual properties. However, very few works pay attention to the dynamic stability of these phases. Here, we examine the potential structures of platinum nitride with a chemical composition of PtN_2 by utilizing a widely adopted evolutionary methodology for crystal structure prediction. Except reproducing the previously proposed phases, we also identify a Pmmm symmetric novel layer structure with a low formation enthalpy that is slightly lower than those of marcasite and $CoSb_2$ structures but slightly higher than that of pyrite structure. The elastic constants and the lattice dynamical calculations show that this layer-structured PtN_2 is mechanically and dynamically stable. The calculated band structures suggest this new phase together with the simple tetragonal phase are metallic, while other phases are insulators. In addition, it is found that the fluorite structure is dynamically unstable by the phonon spectrum calculations, although it is mechanically stable as suggested by calculated elastic constants.

***Keywords**: Noble transition metal nitrides, mechanical properties, electronic property, thermodynamic properties.*

INTRODUCTION

The first successful synthesis of platinum nitride under high-pressure high-temperature (HPHT) in 2004 [1] has stimulated significant interest in noble metal nitrides due to their scientific importance and potential applications. Two more noble metal nitrides, IrN_2 and OsN_2, were synthesized shortly after the discovery of platinum nitride with the same HPHT technique [2–3]. All experiments suggest that these compounds have bulk modulus comparable with those of transitional superhard materials [3] and their structures has stoichiometry XN_2 (X = Pt, Os, Ir) [2]. In 2007, it was reported that the palladium nitride had been synthesized at extreme conditions [4] and ruthenium nitride by reactive pulsed laser ablation [5]. Recently, several novel phases of rhenium nitrides (Re_3N, Re_2N, and ReN_2) have been synthesized and characterized by two different research groups [6–7]. In the following we will restrict our attention on briefly introducing the experimental and theoretical works on platinum nitride solely, including its crystal structure, mechanical and electronic properties.

During the investigation of the firstly synthesized noble metal nitrides, intense works have been focused on its crystal structure initially. As the X-ray diffraction pattern undoubtedly showed that the Pt atoms form a fcc sublattice and therefore authors of [1] suggested the new compound has zinc-blende (space group $F\bar{4}3m$)

structure with Pt : N as 1 : 1. Such opinion has been supported by two theoretical studies [8–9], however, contradicting to that of another first-principles calculation results, which find that this structure is not mechanically stable [10]. Alternatively, the authors of [10] found that platinum nitride can be stabilized in the fluorite structure, in which the nitrogen atoms occupy all the tetrahedral interstitial sites of the metal lattice. Young et al. [11] proposed that the newly synthesized noble metal nitride has the pyrite structure, where single-bonded N_2 units occupy the octahedral interstitial sites of Pt close-packed lattice, resulting in strong and directional Pt–N bonds. Almost at the same time, experimental studies by Crowhurst et al. [2] confirmed that PtN does not exist and that the pyrite structure of PtN_2 is the correct crystal structure. An independent theoretical work by Wessel and Dronskowski [12] reached the same conclusion and emphasized that PtN_2 is incorrectly formulated as "nitride" despite the fact that by definition nitride phase should contain isolated nitrogen and it must be called as platinum pernitride based on the presence of nitrogen dimmers. In 2008, a simple tetragonal structure (*P*4/*mbm*) was predicted to be more thermodynamically stable than the pyrite structure PtN_2 at low pressures and indicated that it can be obtained from marcasite or pyrite structures through martensitic transformation [13]. Yildiz et al. [14] performed a systematic study of the ground state properties of the zinc-blende, rock-salt, tetragonal, cuprite, fluorite, and pyrite phases of platinum nitride. They found that fluorite and pyrite structures are dynamically stable, while the calculated vibration modes of pyrite PtN_2 do not show complete agreement with experimental Raman frequencies. It needs to note that there are also several theoretical works focusing their attention on the marcasite phase of PtN_2 [15, 16], although the commonly accepted opinion is that such phase is the ground state of other noble metal nitrides, like OsN_2 [17–19].

The mechanical properties of platinum mononitride and pernitride have been thoroughly studied as well. In [1] it was determined that the newly synthesized platinum nitride has an extraordinarily high bulk modulus of 372±5 GPa. Most calculated values of bulk modulus of potential platinum nitride crystal structures are smaller than the measured one. Meanwhile, the newly synthesized platinum nitride is unlike traditional transition metal nitrides as it is not superconducting down to 2K and its electronic structure is not very clear [1]. On the one hand, platinum nitride has diverse potential technical applications due to its unique mechanical and electronic properties; on the other hand, progresses in the study of platinum nitride would stimulate related works on other noble metal nitrides and transition metal nitrides, even carbides. Motivated by these issues, in the present work we report a new phase of PtN_2 obtained by ab initio evolutionary algorithm USPEX [20–22].

COMPUTATIONAL PROCEDURE

Variable-cell evolutionary simulations at ambient pressure were performed with USPEX using no experimental information. The systems treated are with 6 atoms, i.e., 2 Pt atoms and 4 N atoms. The first generation of structures was created randomly and the number of structures in the population was set to be 500. The best 60 % of each generation were used to produce the next-generation structures by heredity, softmutation (20 %), randomly from space groups specified (10 %), and the rest are produced by lattice mutation. The best structure of previous generation was set to survive and compete in the following generation. Maximum of 25 generations was required in our global optimization.

In order to calculate the fitness function of each produced structure, USPEX uses VASP [23] as an external ab initio code, where the GGA [24] and the all-electron PAW method [25–26] were adopted. To compare the best structure candidates produced by USPEX and all available potential PtN_2 structures, structure optimizations were performed at a series pressures between 0 and 100 GPa by first-principles methods as implanted in CASTEP code [27]. In these calculations, the LDA [28] was used to describe the exchange and correlation potentials and the plane-wave cut-off energy is set to be 500 eV. For the Brillouin-zone sampling, the Monkhorst-Park scheme [29] with a grid of 0.03 $Å^{-1}$ was adopted. For the self-consistent field iterations, the convergence was assumed when (1) the total energy difference between the last two cycles is less than $5\cdot10^{-6}$ eV/atom; (2) the maximal force on each atom is below 0.01 eV/Å; and (3) the maximal atomic displacement is below $5\cdot10^{-4}$ Å.

RESULTS AND DISCUSSIONS

Crystal structural features and enthalpies

In the present work, we focused on the predicted new phase, Layer structure (space group *Pmmm*: No. 47, hereafter denoted as LS) and the previously proposed potential PtN_2 structures of fluorite [10] (space group *Fm*3*m*: No. 225), pyrite [11] (space group $Pa\bar{3}$: No. 205), marcasite [30, 31] (space group *Pnnm*: No. 58), $CoSb_2$ [30, 31] (space group $P2_1C$: No.14), and a simple tetragonal structure [13] (space group *P*4/*mbm*: No. 127, denoted ST hereafter). In addition, some potential structures proposed for other noble metal nitrides, simple hexagonal (space group *P*6/*mmm*: No. 191, denoted SH hereafter), have also been considered for comparison. All these structures are illustrated in Figs. 1, *a*–*g*. In the fluorite structure, all the N atoms occupy the tetrahedral interstitials of Pt sublattice as shown in Fig. 1, *a*. The fluorite structure is closely related to the pyrite structure with slightly modified fractional coordinates of N atoms [32] (see Table 1). It needs to note that both the fluorite and the pyrite structures are cubic structures. The marcasite structure is orthorhombic, which is widely recognized as the ground state of OsN_2 [33, 34]. In the marcasite structure, the two metal atoms and four nitrogen atoms occupy the 2a and 4g Wyckoff sites, respectively. In addition, the marcasite structure can be considered as an orthorhombic distortion of the cubic pyrite structure. The $CoSb_2$ structure is monoclinic with all of the atoms occupying 4e positions, which is thought to be adopted by the synthesized IrN_2 [34, 35]. Except the fluorite structure, all other aforementioned three structures are composed of PtN_6 octahedra as illustrated in Figs. 1, *b*–*d*. The SH structure contains peculiar double $N=N$ bonded N_2 units (the bond length is 1.179 Å), which was also uncovered for MN_2 (M = Os, Ir, Ru, and Rh) compounds [34]. The LS together with the ST structure proposed in [13] can be considered as layer structures, as their interlayer distance is 2.902 Å and 2.840 Å, respectively. It is necessary to emphasize that the ST structure has also been reproduced by the present setting of evolutionary simulations.

Table 1 lists the calculated lattice parameters, unit cell volumes, densities, and formation enthalpies of PtN_2 with the above mentioned crystal structures. The calculated lattice parameters agree very well with available results, confirming the validity of the adopted simulation approaches. Comparing to pure Pt (ρ = 21.46 g/cm^3), the density of these studied structures reduced significantly owing to the presence of light element N. Among these structures, the pyrite structure has the largest density, while the density of the two layer structures SH and newly uncovered layer structure is less than 50 % of that for pure Pt. Concerning the enthalpies of the studied structures, the ST structure has the lowest enthalpy (ΔH = –0.9622 eV), which is consistent with [13]. The pyrite structure has the second lowest enthalpy (ΔH = –0.7335 eV) and marcasite, $CoSb_2$, and LS have almost equal enthalpies (ΔH = –0.5921, –0.5918, and –0.5977 eV, respectively). Both fluorite and SH structures have positive enthalpies (ΔH = +2.4070 and +0.0023 eV, respectively).

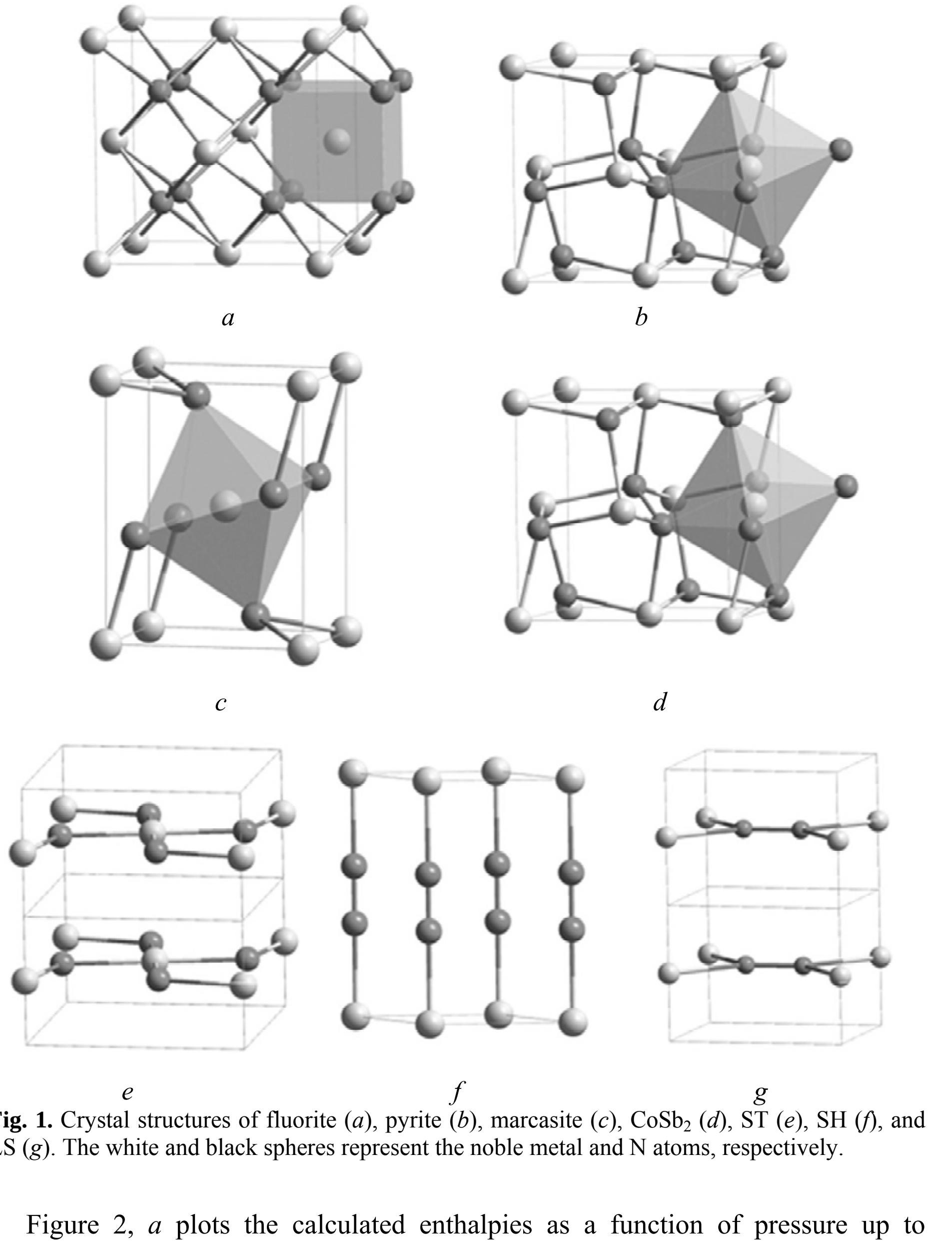

Fig. 1. Crystal structures of fluorite (*a*), pyrite (*b*), marcasite (*c*), $CoSb_2$ (*d*), ST (*e*), SH (*f*), and LS (*g*). The white and black spheres represent the noble metal and N atoms, respectively.

Figure 2, *a* plots the calculated enthalpies as a function of pressure up to 50 GPa for seven studied PtN_2 structures with the enthalpy of the LS PtN_2 as reference. Figure 1, *b* illustrates the formation enthalpies of these seven PtN_2 phases at pressure up to 50 GPa as well. Several interesting features can be inferred from

Table 1. Calculated equilibrium lattice parameters *a*, *b*, *c* (Å), unit cell volume (*V*, Å^3), density (ρ, g/cm^3), formation enthalpy (Δ*H*, eV/formula unit), and band gap (E_g, eV), the available theoretical and experimental values are also listed for comparison, *x* means the value of the fractional coordinates (*x*, *x*, *x*) of N atoms

Structures	*a*	*b*	*c*	β	*x*	*V*	ρ	Δ*H*	E_g
Fluorite	4.9431	–	–	–	0.25	120.78	12.27	+2.4070	–
	4.912[a]					122.28[e]			
	4.939[b]								
	4.963[e]								
Pyrite	4.8258	–	–	–	0.4154	112.39	13.19	–0.7335	1.397
	4.848[b]					118.58[e]			1.5[b]
	4.820[c]								1.66[f]
	4.912[e]								
Marcasite	3.7357	4.8329	3.1693	–	–	57.22	12.95	–0.5921	0.645
	3.736[c]	4.832[c]	3.169[c]	–		–			
	3.779[d]	4.880[d]	3.197[d]	–		58.97[d]			
$CoSb_2$	4.899	4.833	4.899	99.39	–	114	12.95	–0.5918	0.647
	5.460[e]	5.163[e]	9.347[e]	151.2[e]		–			
	4.895[f]	4.833[f]	4.900[f]	99.37[f]		114[f]			
ST	4.8238	4.8238	2.8402	–	–	66.09	11.21	–0.9622	metallic
SH	2.9189	–	5.0055	–	–	36.93	10.03	+0.0023	metallic
LS	2.9021	3.7394	3.1971	–	–	34.70	10.68	–0.5977	metallic
Exp.	4.8041	–	–	–	–	110.88	13.37	–	–

Notes: [a] is the average value from FP-LAPW within LDA and GGA [10]; [b] is PW within PBE [11]; [c] is PW within LDA [36]; [d] is PW within GGA [15]; [e] is spin density functional theory (SDFT) within PBE [37]; [f] is PW within LDA [14].

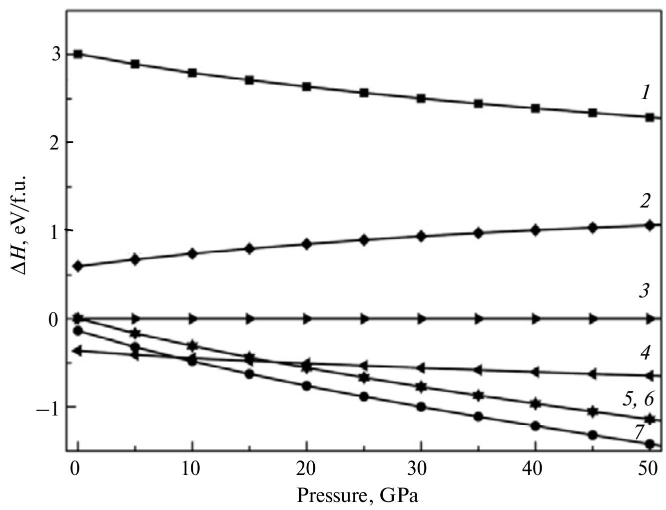

a

Fig. 2. The calculated enthalpies as a function of pressure for the newly discovered phase LS and all available other proposed phases (the enthalpy of the new phase is set to be zero): fluorite (*1*), pyrite (*2*), marcasite (*3*), $CoSb_2$ (*4*), SH (*5*), ST (*6*), LS (7).

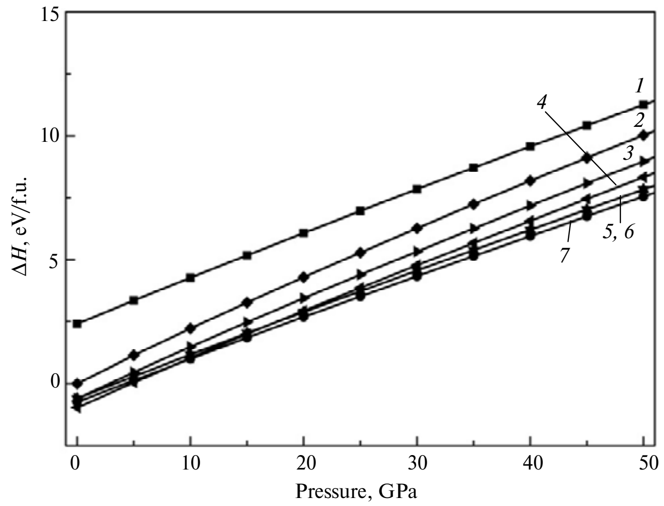

b

Fig. 2. (Contd.)

Fig. 2: (I) the ST phase and the pyrite structure have the lowest and second lowest enthalpies under atmospheric pressure, respectively, marcasite, $CoSb_2$, and the layer-structured phases have almost equal enthalpies, while the SH and fluorite structures have higher enthalpies; (II) when the pressure increases, the stabilities of all these seven phases are gradually decreasing, i.e., their enthalpies are increasing with increasing pressure; (III) the marcasite structure and the $CoSb_2$ structure have almost equal enthalpies in the studied pressure range even up to 100 GPa; (IV) the enthalpies of the LS structure and ST structure have very similar trends under external pressure, possibly owing to that both of them possess layer feature; (V) although the ST structure has the lowest enthalpy under ambient pressure, it becomes less stable than the pyrite structure at about 10 GPa and the marcasite structure and the $CoSb_2$ structure at about 15 GPa; the pyrite structure seems to be the most stable one from about 10 GPa.

Mechanical properties and structural stability

An exotic property of the newly synthesized platinum nitride is its high bulk modulus of 372±5 GPa [1]. As we mentioned in the introduction, most theoretical values of bulk modulus of the proposed platinum nitride crystal structures are smaller than the measured one. For example, the bulk modulus of zinc-blende (ZB) platinum mononitride was calculated to be 194 GPa [8] and 196.3 GPa [10], first-principles calculations with the fully relativistic full potential linearized augmented plane-wave (LAPW) method with and without considering the spin-orbital effect, respectively. In one of our previous works, several approaches have been applied to determine the bulk modulus and elastic constants, including the LAPW method, the plane-wave ultrasoft pseudopotential (PW-PP), and the projected-augmented wave (PAW) methods. The main conclusion is that the platinum nitride in ZB is unstable as the calculated elastic constants $c_{11} < |c_{12}|$ do not fulfill the criteria of mechanical stability. For the fluorite structure, the bulk modulus was calculated to be 316 GPa and 264 GPa, depending on the use of local density approximation (LDA) and the generalized gradient approximation (GGA) exchange correlation functional, respectively [10]. According to [11], the bulk modulus of PtN_2 having pyrite structure is 305 GPa within the density functional theory using a Perdew-

Burke-Ernzerhoff (PBE) exchange correlation function. The bulk modulus of marcasite PtN_2 is calculated to be 362 GPa by its relation to elastic constants and 352 GPa by fitting to a third order Birch-Murnaghan equation of state [10], respectively. The Young's modulus (E), shear modulus (G) and Poisson's ratio (ν) of ZB, fluorite, pyrite structure of platinum nitride have also been studied as done in [11]. The low value of Poisson's ratio and the high G/B ratio suggests a high degree of covalency, implying that intercalation of the dinitrogen units into the Pt lattice induces a substantial change of the electronic from metallic in bulk Pt to covalent PtN_2. Gou et al. [36] have calculated the hardness values of both the cubic pyrite and orthorhombic FeS_2 structure PtN_2 based on Mulliken overlap population analysis in first-principles technique, which are 16.0 and 6.4 GPa, respectively. The hardness of the pyrite-type PtN_2 is close to that of TiN (18 GPa), indicating that it has excellent mechanical properties and possesses potential technological and industrial applications.

In Table 2 we listed the elastic properties and bulk modulus of the new discovered phase as well as all other available phases. From the present work the bulk modulus of PtN_2 fluorite structure is slightly smaller than those of pyrite and marcasite structures. However, all of them are at least 10 % smaller than the experimental value of bulk modulus. Although there is one theoretical work [36] that reports a value of 361 GPa of bulk modulus for the pyrite PtN_2, other theoretical works do not support it [11, 31, 37]. The bulk modulus of the later $CoSb_2$ structure is comparable to that of fluorite structure. Not very surprisingly, the bulk modulus of the recently discovered phases including the one found in the present work is much smaller than those of other phases and the experimental value.

Table 2. Calculated elastic constants, bulk and shear moduli (all in GPa) of the newly discovered phase and all available other proposed phases

	c_{11}	c_{22}	c_{33}	c_{44}	c_{55}	c_{66}	c_{12}	c_{13}	c_{15}	c_{23}	c_{25}	c_{35}	c_{46}	B	G
Fluorite	480	–	–	95	–	–	229	–	–	–	–	–	–	313	106
	495[a]			111[a]			188[a]							294[a]	
	473[b]			115[b]			160[b]							264[b]	
Pyrite	791	–	–	132	–	–	102	–	–	–	–	–	–	332	196
	696[b]			136[b]			83[b]							288[b]	221[b]
	842[c]			152[c]			120[c]							361[c]	236[c]
Marcasite	569	779	555	103	300	146	111	304	–	106	–	–	–	327	183
	545[c]	798[c]	550[c]	111[c]	295[c]	159[c]	121[c]	310[c]		116[c]				331[c]	203[c]
$CoSb_2$	754	850	753	148	133	145	119	150	–5	117	15	53	–15	344	198
	729[e]	822[e]	724[e]	141[e]	138[e]	130[e]	126[e]	157[e]	–50[e]	129[e]	–2[e]	59[e]	–20[e]	344[e]	–
ST	906	–	144	22	–	156	161	14	–	–	–	–	–	118	101
SH	75	–	1291	33	–	–	103	65	–	–	–	–	–	89	13
LS	110	647	634	277	17	15	22	32	–	359	–	–	–	97	80

Notes: [a] is the average values from FP-LAPW within LDA and GGA [10]; [b] is PW within PBE [11]; [c] is PW within LDA [36]; [d] is PW within GGA [15]; [e] PW is within LDA [30].

Now, let us turn our attention to the elastic constants of these phases of PtN_2. From the calculated elastic constants one can not only obtain the bulk and shear moduli as done in the present work but can know the mechanical stability of the studied system. For a cubic structure, it needs to note that one can also get the bulk modulus and its pressure derivative by fitting the calculated p–V data by using the third Birch-Murnaghan equation of state [10, 38]. For the LS phase, the bulk modulus obtained by this way is 109 GPa, which is in good agreement with that calculated by elastic constants. The key criterion for mechanical stability of a crystal is that the strain energy must be positive [39], which means, for a cubic crystal, that the elastic constants should satisfy the following inequalities

$$c_{44} > 0,\ c_{11} > |c_{12}|,\ c_{11} + 2c_{12} > 0, \tag{1}$$

for orthorhombic crystals

$$c_{11} + c_{22} - c_{12} > 0,\ c_{11} + c_{33} - c_{23} > 0,\ c_{22} + c_{33} - c_{23} > 0, \tag{2}$$

for a hexagonal crystal

$$c_{44} > 0,\ c_{11} > |c_{12}|,\ (c_{11} + c_{12})c_{33} > 2c_{13}^2, \tag{3}$$

for a tetragonal crystal

$$\begin{gathered} c_{11} > 0,\ c_{33} > 0,\ c_{44} > 0,\ c_{66} > 0,\ (c_{11} - c_{12}) > 0; \\ (c_{11} + c_{33} - 2c_{13}) > 0,\ [2(c_{11} + c_{12}) + c_{33} + 4c_{13}] > 0, \end{gathered} \tag{4}$$

and for monoclinic

$$\begin{gathered} c_{11} > 0,\ c_{22} > 0,\ c_{33} > 0,\ c_{44} > 0,\ c_{55} > 0,\ c_{66} > 0; \\ [c_{11} + c_{22} + c_{33} + 2(c_{12} + c_{13} + c_{23})] > 0,\ (c_{44}c_{66} - c_{46}^2) > 0,\ (c_{22} + c_{33} - 2c_{23}) > 0; \\ 2[c_{15}c_{25}(c_{33}c_{12} - c_{13}c_{23}) + c_{15}c_{35}(c_{22}c_{13} - c_{12}c_{23}) + c_{25}c_{35}(c_{11}c_{23} - c_{12}c_{13})] - \\ -[c_{15}^2(c_{22}c_{33} - c_{23}^2) + c_{25}^2(c_{11}c_{33} - c_{13}^2) + c_{35}^2(c_{11}c_{22} - c_{12}^2)] + c_{55}^4 > 0. \end{gathered} \tag{5}$$

The calculated elastic constants of seven studied structures are listed in Table 2. As we mentioned, fluorite and pyrite structures are cubic and their elastic constants satisfy expression (1). The marcasite and the new uncovered structures are orthorhombic and their elastic constants should satisfy expression (2). The SH structure is hexagonal, the ST structure is tetragonal and the $CoSb_2$ structure is monoclinic, therefore they are determined to be mechanically stable as their calculated elastic constants satisfy expressions (3), (4), and (5), respectively. Obviously, all these proposed PtN_2 structures are mechanically stable.

In order to clarify if these structures are dynamically stable, the phonon dispersion curves and phonon density of states have been calculated based on the finite displacement algorithms as coded in the CASTEP module of the Materials Studio package, where the phonon frequencies can be obtained with the finite displacement method without creating a supercell. In Fig. 3, the phonon dispersion curves of all found phases are demonstrated. The calculated results reveal that all these studied phases except the fluorite and the SH structures are dynamically stable. For the fluorite structure, it is very clear that there is a strong imaginary phonon frequency along the M–G direction in the Brillouin zone, which is contrary to the conclusion of Yildiz et al. [14]. In their work, only the phonon dispersion of the pyrite structure was plotted, which is in agreement with the present work. However, the calculated phonon dispersion of the fluorite structure was not illustrated for comparison. Therefore, we have repeated the phonon dispersion calculations with the supercell displacements approach as implemented in the phonopy code [40] for the fluorite and LS structures, confirming that the fluorite structure is dynamically unstable and the LS structure is dynamically stable.

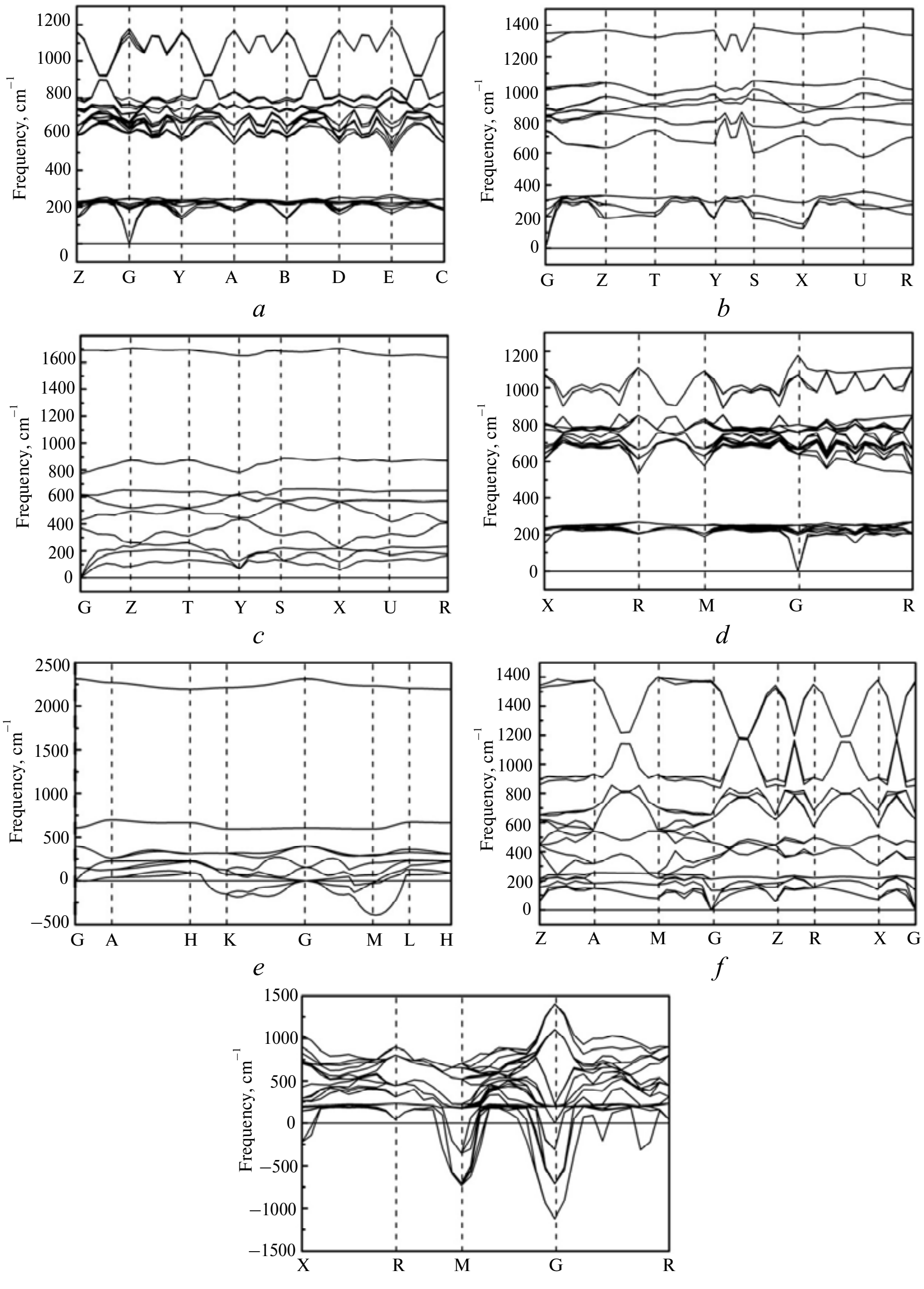

Fig. 3. Phonon dispersion curves for PtN_2 with different structures: $CoSb_2$ (*a*), marcasite (*b*), LS (*c*), pyrite (*d*), SH (*e*), ST (*f*), flourite (*g*).

Electronic properties

Many efforts have been devoted to characterize the electronic structures and bonding nature. As mentioned before, it was determined that the newly synthesized platinum nitride is unlike traditional transition metal nitrides VN and NbN as it is not superconducting down to 2 K and one could not tell whether it is a poor metal or a narrow gap semiconductor. Theoretically, Wessel et al. [12] studied the N–N bonding and the metal oxidation state in PtN_2. The N–N distances of N_2 unit in PtN_2 is 1.41 Å, matches very well with the F–F distance 1.42 Å. It needs to emphasize that the fluorine molecule is isoelectronic with N_2^{4-}. The bond-length considerations and spectroscopic results in combination with molecular-orbital arguments clearly support a single-bonded $(N–N)^{4-}$ unit in PtN_2. It was found that the fluorite structure of PtN_2 has a pseudogap feature, which was used to explain its mechanical stability [10]. The electronic structure of the pyrite structure has also been studied by several groups, and an indirect band gap is found to be about 1.5 eV using GGA-PBE exchange correlation function [11] or 1.66 eV in the framework of LDA [14]. Chen et al. have investigated the electronic structures of pyrite, marcasite and $CoSb_2$ and found that all of them are insulators [31]. Soto [41] has systematically studied the heavy-metal pernitrides using LAPW methods. He proposed that the strong covalent N–N bond, the ionic character of Metal–N bonds and the metal–metal distances all contribute to the high bulk modulus of transition metal pernitrides. Very recently, the geometries, phase stabilities and electronic properties of bulk Pt_3N, PtN, and PtN_2 have been investigated in a set of twenty different crystal structures [37].

In the present work, we have systematically investigated the band structures of dynamically stable PtN_2 in pyrite, marcasite, $CoSb_2$, ST and LS structures. The calculated band structures are given in Figs. 4a–4e and the values of band gap are listed in the last column of Table 1. The band gap of pyrite structure is 1.397 eV, which is in good agreement with other works [11, 14], implying the validity of the algorithms adopted here. The band gaps of marcasite and $CoSb_2$ structure are 0.645 and 0.647 eV, respectively, confirming their insulator character [31]. Interestingly, the calculated band structures suggest that the newly discovered layer phase together with the ST phase are both metallic. In order to further study the bonding character of the new phase, its electron density difference (EDD) is calculated and shown in Fig. 5. As is well known, the EDD can illustrate the charge redistribution due to chemical bonding. It is clearly seen that the EDD between Pt and N atoms is biased toward the N atoms, indicating a partially covalent bonding, which is a very common feature among noble metal nitrides. However, the localization of EDD between the N–N pairs seems quite different from that of pyrite structure of PtN_2 as shown by the EDD in Fig. 4 of Ref. [11]. Such strong electron transfer between the single-bonded N_2 units may explain the conductance of the new structure of PtN_2, while other structures like pyrite and marcasite that also contain N_2 units were reported to be insulating.

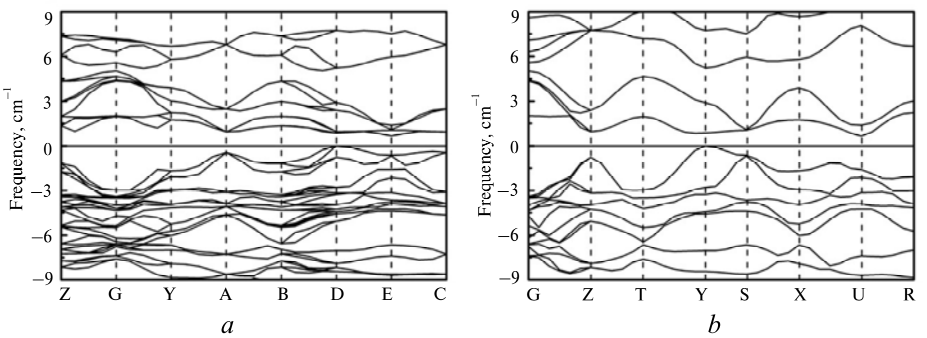

Fig. 4. Band structures for PtN_2 with different structures: $CoSb_2$ (*a*), marcasite (*b*), LS (*c*), pyrite (*d*), ST (*e*).

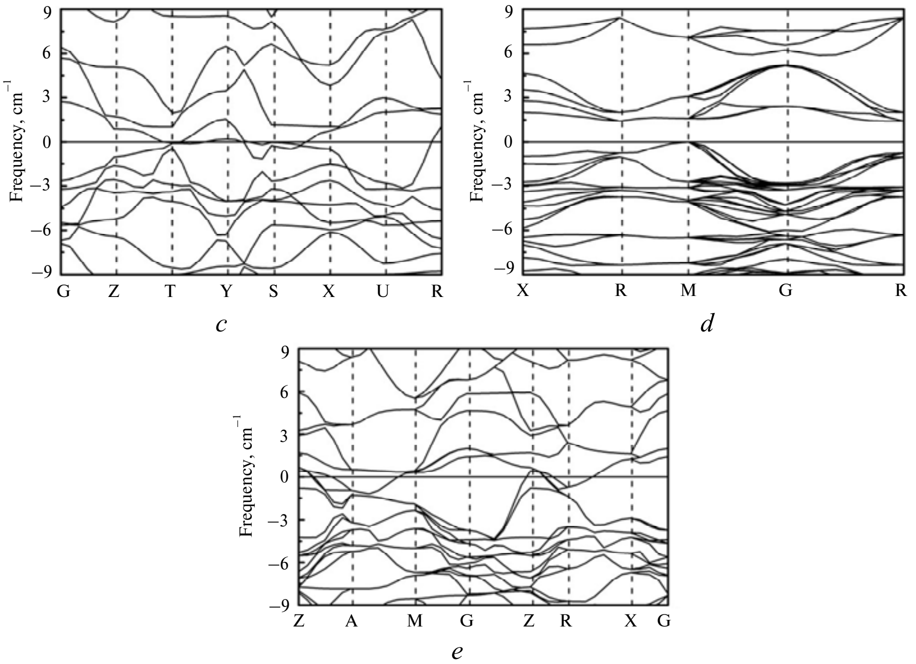

Fig. 4. (Contd.)

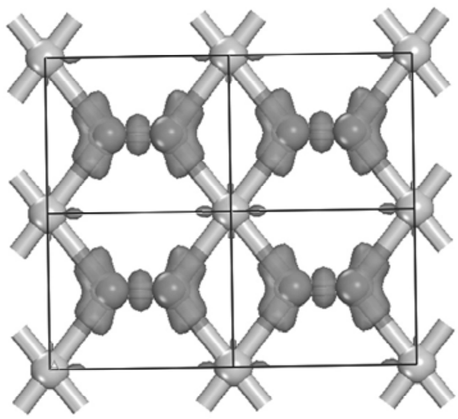

Fig. 5. Different electronic densities for PtN_2 in the newly discovered layer LS phase.

CONCLUSIONS

In summary, a novel layer structure of PtN_2 with space group Pmmm has been discovered by evolutionary methodology for crystal structure prediction. The new phase is found to be mechanically and dynamically stable, and has a low formation enthalpy. Band structure calculations show that it is metallic and may be explained by the special localized electron density between the single-bonded N_2 units as shown by the calculated electron density difference. The calculated elastic constants and Debye temperature imply that the new phase is neither very hard nor very soft. It has also been found that the fluorite structure is dynamically unstable and the ST phase is also metallic. The pyrite and the $CoSb_2$ structures of PtN_2 could be very hard because they have considerably larger bulk modulus than those of other studied phases. The present work may stimulate further experimental or theoretical works on investigating the synthesis and properties of noble metal compounds.

This work was supported by the NSFC (Grants Nos. 51121061 and 51271160), which is gratefully acknowledged. ZSZ's fellowship is supported by Energy Frontier Research in Extreme Environments Center (EFree), an Energy Frontier Research Center funded by the U.S. Department of Energy, Office of Science under Award Number DE-SC0001057.

Розглянуто потенційні структури нітриду платини з хімічним складом PtN_2, використовуючи широко прийняту еволюційну методологію прогнозування кристалічних структур. Крім відтворення раніше запропонованих фаз, ідентифіковано нову симетричну шарувату структуру, просторова група Pmmm, з низькою ентальпією формування, яка трохи менша, ніж ентальпії структур марказиту і $CoSb_2$, але дещо більша, ніж ентальпія структури піриту. Постійні пружності і динамічні розрахунки решітки показують, що цей нітрид платини (PtN_2) з шаруватою структурою механічно і динамічно стабільний. Розраховані зонні структури дозволяють припустити, що ця нова фаза разом з простою тетрагональною фазою є металічною, тоді як інші фази є діелектричні. Розрахунками фононного спектру встановлено, що структура флюориту динамічно нестабільна, хоча механічно стабільна, як передбачається розрахованими константами пружності.

Ключові слова: *нітриди перехідних благородних металів, механічні властивості, електронні властивості, термодинамічні властивості.*

Рассмотрены потенциальные структуры нитрида платины с химическим составом PtN_2, используя широко принятую эволюционную методологию прогнозирования кристаллических структур. Кроме воспроизведения ранее предложенных фаз, идентифицировано новую симметричную слоистую структуру, пространственная группа Pmmm, с низкой энтальпией формирования, которая немного меньше, чем энтальпии структур марказита и $CoSb_2$, но немного больше, чем энтальпия структуры пирита. Постоянные упругости и динамические расчеты решетки показывают, что этот нитрид платины (PtN_2) со слоистой структурой механически и динамически стабилен. Рассчитанные зонные структуры позволяют предположить, что эта новая фаза вместе с простой тетрагональной фазой является металлической, тогда как другие фазы являются диэлектрическими. Расчетами фононного спектра установлено, что структура флюорита динамически нестабильна, хотя механически стабильна, как предполагается рассчитанными константами упругости.

Ключевые слова: *нитриды переходных благородных металлов, механические свойства, электронные свойства, термодинамические свойства.*

1. *Gregoryanz E., Sanloup C., Somayazulu M. et al.* Synthesis and characterization of a binary noble metal nitride // Nature Mater. – 2004. – **3**. – P. 294–297.
2. *Crowhurst J. C., Goncharov A. F., Sadigh B. et al.* Synthesis and characterization of the nitrides of platinum and iridium // Science. – 2006. – **311**, N 5765. – P. 1275–1278.
3. *Young A. F., Sanloup C., Gregoryanz E. et al.* Synthesis of novel transition metal nitrides IrN_2 and OsN_2 // Phys. Rev. Lett. – 2006. – **96**, art. 155501.
4. *Crowhurst J. C., Goncharov A. F., Sadigh B. et al.* Synthesis and characterization of nitrides of iridium and palladium // Mater. Res. Soc. – 2007. – **987**. – P. 03–09.
5. *Moreno-Armenta M. G., Diaz J., Martinez-Ruiz A., Soto G.* Synthesis of cubic ruthenium nitride by reactive pulsed laser ablation // J. Phys. Chem. Solids. – 2007. – **68**, N 10. – P. 1989–1994.
6. *Friedrich A., Winkler B., Bayarjargal L. et al.* Novel rhenium nitrides // Phys. Rev. Lett. – 2010. – **105**, art. 085504.
7. *Kawamura F., Yusa H., Taniguchi T.* Synthesis of rhenium nitride crystals with MoS_2 structure // Appl. Phys. Lett. – 2012. – **100**, art. 251910.
8. *Sahu B. R., Kleinman L.* PtN: a zinc-blende metallic transition-metal compound // Phys. Rev. B. – 2005. – **71**, art. 041101.
9. *Uddin J., Scuseria G. E.* Structures and electronic properties of platinum nitride by density functional theory // Ibid. – 2005. – **72**, art. 035101.
10. *Yu R., Zhang X. F.* Platinum nitride with fluorite structure // Appl. Phys. Lett. – 2005. – **86**, art. 121913.

11. *Young A. F., Montoya J. A., Sanloup C. et al.* Interstitial dinitrogen makes PtN_2 an insulating hard solid // Phys. Rev. B. – 2006. – **73**. – P. 153102.
12. *Wessel M., Dronskowski R.* Nature of N−N bonding within high-pressure noble-metal pernitrides and the prediction of lanthanum pernitride // J. Am. Chem. Soc. – 2012. – **132**. – P. 2421–2429.
13. *Åberg D., Sadigh B., Crowhurst J., Goncharov A. F.* Thermodynamic ground states of platinum metal nitrides // Phys. Rev. Lett. – 2008. – **100**, art. 095501.
14. *Yildiz A., AkinciÜ., Gülseren O., Sökmen İ.* Characterization of platinum nitride from first-principles calculations // J. Phys.: Condens. Matter. – 2009. – **21**, art. 485403.
15. *Chen Z. W., Guo X. J., Liu Z. Y. et al*. Crystal structure and physical properties of OsN_2 and PtN_2 in the marcasite phase // Phys. Rev. B. – 2007. – **75**, art. 054103.
16. *Zhu Y., Fan C. Z., Zhang X. Y. et al.* Theoretical study of the properties of PtN_2 with pyrite and marcasite structures // Solid State Commun. – 2009. – **149**, N 25–26. – P. 1021–1024.
17. *Montoya J. A., Hernández A. D., Sanloup C. et al*. OsN_2 Crystal structure and electronic properties // Appl. Phys. Lett. – 2007. – **90**, art. 011909.
18. *Wang Y. X., Arai M., Sasaki T.* Marcasite osmium nitride with high bulk modulus: First-principles // Ibid. – 2007. – **90**, art. 061922.
19. *Hernández E. R., Canadell E.* Marcasite vs. arsenopyrite structural choice in MN_2 (M = Ir, Os and Rh) transition metal nitrides // J. Mater. Chem. – 2008. – **18**. – P. 2090–2095.
20. *Oganov A. R., Glass C. W.* Crystal structure prediction using *ab initio* evolutionary techniques: principles and applications // J. Chem. Phys. – 2006. – **124**, art. 2444704.
21. *Glass C. W., Oganov A. R., Hansen N.* USPEX–Evolutionary crystal structure prediction // Computer Phys. Commun. – 2006. – **175**, N 11–12. – P. 713–720.
22. *Zhu Q., Oganov A. R., Glass C. W., Stokes H. T.* Constrained evolutionary algorithm for structure prediction of molecular crystals: methodology and applications // Acta Crystallogr., Sect. B: Struct. Sci. – 2012. – **68**. – P. 215–226.
23. *Kresse G., Furthmüller J.* Efficient iterative schemes for *ab initio* total-energy calculations using a plane-wave basis set // Phys. Rev. B. – 1996. – **54**. – P. 11169–11186.
24. *Perdew J. P., Burke K., Ernzerhof M.* Generalized gradient approximation made simple // Phys. Rev. Lett. – 1996. – **77**. – P. 3865–3868.
25. *Blöchl P. E.* Projector augmented-wave method // Phys. Rev. B. – 1994. – **50**. – P. 17953–17979.
26. *Kresse G., Joubert D.* From ultrasoft pseudopotentials to the projector augmented-wave method // Ibid. – 1999. – **59**. – P. 1758–1775.
27. *Segall M. D., Linda P. L. D., Probert M. J. et al.* First-principles simulation: ideas, illustrations and the CASTEP code // J. Phys.: Condens. Matter. – 2002. – **14**, N 11. – P. 2717–2744.
28. *Ceperley D. M., Alder B. J.* Ground state of the electron gas by a stochastic method // Phys. Rev. Lett. – 1980. – **45**. – P. 566–569.
29. *Monkhorst H. J., Pack J. D*. Special points for Brillouin-zone integrations // Phys. Rev. B. – 1976. – **13**. – P. 5188–5192.
30. *Chen W., Jiang J. Z.* Elastic properties and electronic structures of 4d- and 5d-transition metal Mononitrides // J. Alloys Compd. – 2010. – **499**, N 2. – P. 243–254.
31. *Chen W., Tse J. S., Jiang J. Z.* An *ab initio* study of 5d noble metal nitrides: OsN2, IrN_2, PtN_2 and AuN_2 // Solid State Commun. – 2010. – **150**, N 3–4. – P. 181–186.
32. *Yu R., Zhan Q., Zhang X. F.* Elastic stability and electronic structure of pyrite type PtN_2: A hard semiconductor // Appl. Phys. Lett. – 2006. – **88**, art. 051913.
33. *Wu Z. J., Zhao E. J., Xiang H. P. et al.* Crystal structures and elastic properties of superhard IrN_2 and IrN_3 from first principles // Phys. Rev. B. – 2007. – **76**, art. 054115.
34. *Li Y. W., Wang H., Li Q. et al.* Twofold coordinated ground-state and eightfold high-pressure phase of heavy transition metal nitrides MN_2 (M = Os, Ir, Ru, and Rh) // Inorg. Chem. – 2009. – **48**. – P. 9904–9909.
35. *Wu Z. J., Hao X. F., Liu X. J., Meng J.* Structures and elastic properties of OsN_2 investigated via first-principles density functional calculations // Phys. Rev. B. – 2007. – **75**, art. 054115.
36. *Gou H. Y., Hou L., Zhang J. W. et al.* First-principles study of low compressibility osmium borides // Appl. Phys. Lett. – 2006. – **88**, art. 221910.
37. *Suleiman M. S. H., Joubert D. P.* Structural, electronic and optical characterization of bulk platinum nitrides: a first-principles study // arXiv: 1301.5490 v1 [cond-mat.mtrl-sci].
38. *Liu Q. X., Fan C. Z., Zhang R. J.* First-principles study of high-pressure structural phase transitions of Magnesium // J. Appl. Phys. – 2009. – **105**, art. 123505 (4 p.).

39. *Nye J. F.* The stress tensor // Phys. Properties Crystals. – Oxford: Oxford University Press, 1985. – P. 82–93.
40. *Togo A., Oba F., Tanaka I.* First-principles calculations of the ferroelastic transition between rutile-type and $CaCl_2$-type SiO_2 at high pressures // Phys. Rev. B. – 2008. – **78**, art. 134106.
41. *Soto G.* Computational study of Hf, Ta, W, Re, Ir, Os and Pt pernitrides // Comp. Mater. Sci. – 2012. – **61**. – P. 1–5.

State Key Laboratory of Metastable Materials
Science and Technology, Yanshan University
Geophysical Laboratory, Carnegie Institution of Washington, USA

Received July 29, 2013